Creep, Stress Relaxation, and Plastic Deformation in Sn-Ag and Sn-Zn Eutectic Solders

H. MAVOORI, J. CHIN, S. VAYNMAN, B. MORAN, L. KEER, and M. FINE
Northwestern University, Evanston IL 60208

Because of the high homologous operation temperature of solders used in electronic devices, time and temperature dependent relaxation and creep processes affect their mechanical behavior. In this paper, two eutectic lead-free solders (96.5Sn–3.5Ag and 91Sn–9Zn) are investigated for their creep and stress relaxation behavior. The creep tests were done in load-control with initial stresses in the range of 10–22 MPa at two temperatures, 25 and 80°C. The stress relaxation tests were performed under constant-strain conditions with strains in the range of 0.3–2.4% and at 25 and 80°C. Since creep/relaxation processes are active even during monotonic tensile tests at ambient temperatures, stress-strain curves at different temperatures and strain rates provide insight into these processes. Activation energies obtained from the monotonic tensile, stress relaxation, and creep tests are compared and discussed in light of the governing mechanisms. These data along with creep exponents, strain rate sensitivities and damage mechanisms are useful for aiding the modeling of solder interconnects for reliability and lifetime prediction. Constitutive modeling for creep and stress relaxation behavior was done using a formulation based on unified creep plasticity theory which has been previously employed in the modeling of high temperature superalloys with satisfactory results.

Key words: Creep, constitutive modeling, Sn-Ag eutectic, Sn-Zn eutectic, solders, stress relaxation

INTRODUCTION

When a material is mechanically deformed at a high homologous temperature, thermally activated plastic flow plays a dominant role even though athermal dislocation glide processes also play a role. Thermally activated plastic flow mechanisms are characterized by stress exponents and activation energies. The present paper compares the activation energies and stress exponents obtained for Sn-Ag and Sn-Zn eutectic solders for creep, stress relaxation and monotonic stress-strain relations at 25 and 80°C, a high homologous temperature for these materials.

The creep mechanisms which may be active are: dislocation climb (characterized by a stress exponent of 6–7 and an activation energy corresponding to self-diffusion), viscous dislocation glide (characterized by a stress exponent of 3–4) and grain boundary sliding (characterized by a stress exponent of 2–3 and an activation energy corresponding to grain-boundary diffusion). The pre-exponential factor of the power law equation [A in Eq. (1)] includes microstructural effects.[1] Tribula and Morris observed that lower stress exponents correspond to uniform deformation without apparent local microstructural instability.[2] Grain boundary sliding results in intergranular failure while the other mechanisms lead to grain deformation. In the case of multi-phase materials with large volume fractions of phases, interphase boundary sliding may act similar to grain boundary sliding. As the strain rate is increased or the temperature is lowered, stress-strain behavior becomes increasingly less dependent on thermally activated processes. A hierarchy of increasing activation energy processes is expected giving rise to a hierarchy of time constants. Since grain boundary sliding has a higher strain rate sensitivity than matrix plastic flow, grain boundaries become preferentially slippery at low strain rates. In polycrystalline materials, near triple points it is necessary for the matrix to deform in order to accommodate sliding and hence although most of the deformation occurs by grain boundary sliding, matrix creep may

(Received January 8, 1997; accepted March 3, 1997)

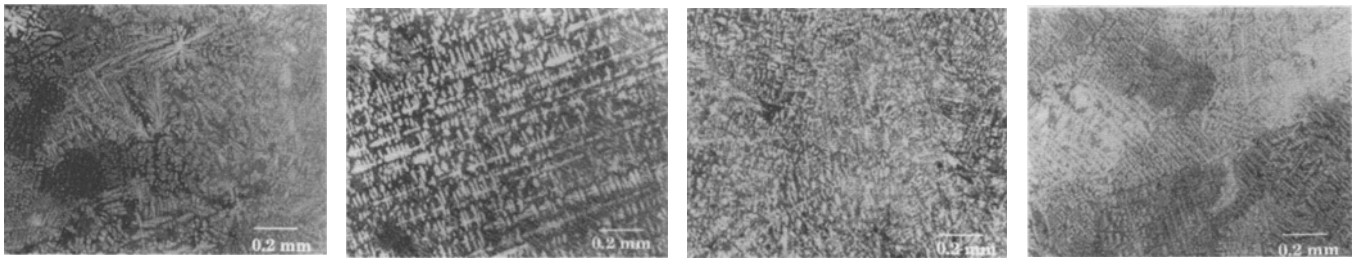

Fig. 1. Microstructures: (a) original as-cast undeformed Sn-Ag eutectic (b) after tensile testing, (c) stress relaxation, and (d) creep.

become rate limiting.[3] In tensile tests, the stress at a given strain increases with strain rate. Due to the time dependence of thermally activated processes like creep, a higher strain rate allows less time for creep strains leading to a higher strength.[4]

In thermomechanical fatigue, at high homologous temperatures, both thermal and athermal processes are active. At low strain rates or high temperatures, creep dominates; however, at high frequencies or low temperatures, failure is dominated by athermal processes as creep has little time to act. During the cold part of a thermomechanical fatigue cycle, there is less stress relaxation than during the higher temperature part of the cycle due to lower thermal energy. Fracture relieves unrelaxed thermal stresses caused by coefficient of expansion mismatch among components.[5]

At high homologous temperatures, tensile and stress relaxation tests allow a wide range of stress and temperature conditions to be studied quickly. In stress relaxation tests, the same specimen may be used for several sets of conditions due to the small accumulation of plastic strain for each measurement. During stress relaxation tests, the deformation processes involved are closely representative of those in an actual solder joint during the temperature hold periods of the actual thermomechanical cycle during operation of the electronic device. This is not the case for steady state creep tests and they are more time consuming. This makes stress relaxation and tensile tests more suitable for reliability modeling than creep tests.[6] An analysis of stress relaxation curves can yield stress exponents, dislocation velocities, thermal and athermal components of flow stress and plastic flow related thermodynamic parameters like activation energies and activation volumes.[7] Further, analysis of the tensile test data vs temperature and strain rate gives further information about these properties and the operative flow and fracture mechanisms.

In this paper, tensile, stress relaxation and creep data obtained on bulk cast samples of two eutectic solders, 96.5Sn–3.5Ag and 91Sn–9Zn (compositions in weight percent), are analyzed to obtain activation energy and stress exponent information and the results of the different tests are compared. Further tensile test curves vs strain rate allow establishment of an approximate athermal stress strain curve. Since two formulations of the power law are used in literature (one with a temperature term in the pre-exponent and one without) both are compared [see Eq. (1) and Eq. (3)]. A linear regression analysis based on minimizing root mean square error similar to that used by Mei and Morris[8] was used to obtain the material parameters.

Creep and stress relaxation can be modeled well by the unified creep plasticity model proposed by McDowell et al.[9] It is able to account for residual stress in stress relaxation and should be useful in incorporating time-dependent effects into numerical techniques for solder joint analysis and reliability prediction.

The microstructure of the original as-cast undeformed Sn-Ag eutectic is shown in Fig. 1a. The microstructures after tensile testing, stress relaxation and creep are shown in Figs. 1b, 1c, and 1d, respectively. In these micrographs, the light etching phase is β–Sn. Before testing the β–Sn dendrites are rather random in orientation. Tensile deformation fragmented the dendrites and oriented the β-Sn fragments along lines of approximately 45° to the load direction. After stress relaxation following tensile deformation, the β-Sn phase particles have reoriented into columns. The alignment in the maximum shear direction has been lost. The structure after creep contains β-Sn dendrites also reduced in size from the original casting. Some dendrites are aligned at 45° to the tensile axis but the structure is less oriented than after tensile deformation.

STRESS VS STRAIN RATE RELATIONS

A commonly used equation by design engineers for stress and temperature dependence of creep strain rate, especially in the electronics industry, is the Norton power law:[10]

$$\dot{\varepsilon} = A\sigma^n \exp\left(\frac{-Q}{RT}\right) \tag{1}$$

where $\dot{\varepsilon}$ is the steady state creep strain rate, A is a constant, σ is the stress, n is the stress exponent, Q is the activation energy, R is the universal gas constant, and T is the absolute temperature.

Favored by researchers of creep behavior is the general Dorn equation[11] that describes high homologous temperature steady-state plastic deformation:

$$\frac{\dot{\varepsilon}RT}{D\mu b} = C\left(\frac{\sigma}{\mu}\right)^n \left(\frac{b}{d}\right)^p \tag{2}$$

Table I. Flow Stresses in MPa at 5% Total Strain and Different Strain Rates from Monotonic Tensile Curves for 96.5Sn–3.5Ag and 91Sn–9Zn

	96.5Sn-3.5Ag		91Sn-9Zn	
Strain Rate (s–1)	25°C	80°C	25°C	80°C
0.01	39.4	23.0	62.3	28.7
0.001	32.8	17.5	48.4	22.0
0.0001	26.3	16.0	37.5	17.5
0.00001	23.0	12.5	26.5	12.0

where D is the appropriate diffusion coefficient, μ is the shear modulus, b is the Burgers vector, C and p are constants, and d is the grain size or interphase spacing.

Using $D = D_0 \exp(-Q/RT)$ where D_0 is a constant, Eq. (2) can be rewritten as:

$$\dot{\varepsilon} = A\frac{\sigma^n}{T}\exp\left(\frac{-Q}{RT}\right) \quad (3)$$

where A is taken to be a constant. It is to be noted that the form of Eq. (3) differs from Eq. (1) by a factor of 1/T. The shear modulus, of course, decreases on heating imparting a temperature dependence to A. The T term in the exponential is much more important than the pre-exponential 1/T and the small decrease in modulus on heating.

For some phenomena, the introduction of a "friction" stress or "threshold" stress σ_t is necessary to get reasonable values of n and Q. The threshold stress formulation of the Norton power law [Eq. (1)] can then be written as:

$$\dot{\varepsilon} = A(\sigma - \sigma_t)^n \exp\left(\frac{-Q}{RT}\right) \quad (4)$$

where σ_t is the threshold stress.

EXPERIMENTS

Bulk, cast, dog-bone shaped specimens with rectangular cross-sections were used for all tests. The gage section dimensions were 12 × 12.5 × 6.5 mm. The objective was to establish a general material properties database which could provide inputs to models for specific geometries of interest. After casting and machining, the specimens were heat-treated at 150°C for 24 h followed by aging at room temperature for 6–10 days to stabilize the microstructure. The testing was done on a servo-hydraulic MTS machine controlled by a 458.20 programmable microconsole. Temperature control was through heated grips with thermocouple feedback to a microprocessor based thermal controller. The tensile and stress relaxation tests were performed in strain-control while the creep tests were run in load control.

Tensile Tests

The monotonic tensile test results for 96.5Sn–3.5Ag and 91Sn–9Zn were published previously[16] but are given here for completeness. They were carried out in strain control at strain rates ranging from 10^{-5} to 10^{-2} per s and two temperatures 25 and 80°C. The strain was increased linearly at a constant rate and the stress was monitored. The engineering stress-strain curves obtained are shown in Figs. 2a and 2b.

The flow stresses at corresponding strains in both Sn-Ag and Sn-Zn eutectic solders are strong functions of strain rate at 25 and 80°C with the stresses increasing with increasing strain rate (Table I) due to less

Table II. Strain Rate Sensitivities of 96.5Sn–3.5Ag and 91Sn–9Zn

Material	Temp.(°C)	m
96.5Sn–3.5Ag	25	0.080
96.5Sn–3.5Ag	80	0.083
91Sn–9Zn	25	0.122
91Sn–9Zn	80	0.124

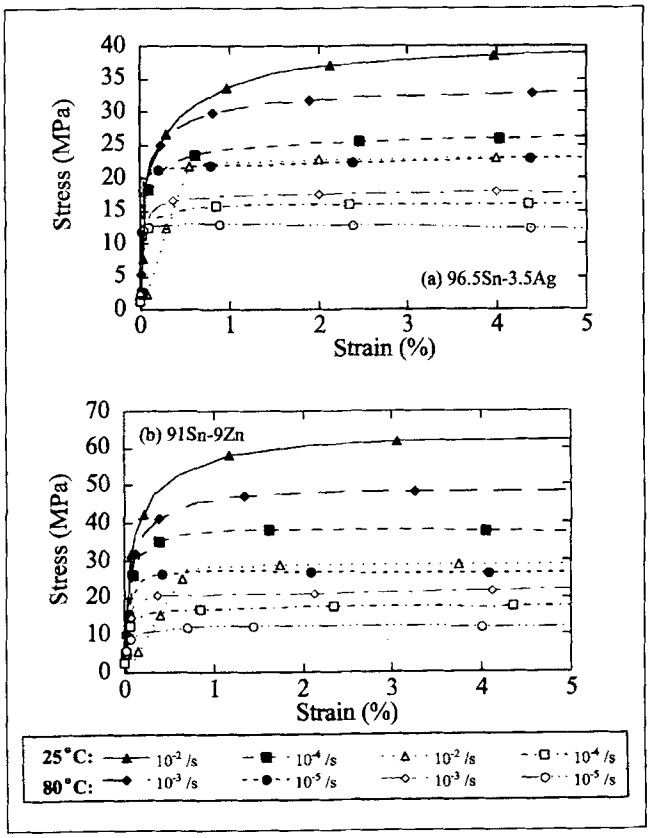

Fig. 2. Tensile test curves at different strain rates and temperatures for (a) 96.5Sn–3.5Ag, and (b) 91Sn-9Zn.[16]

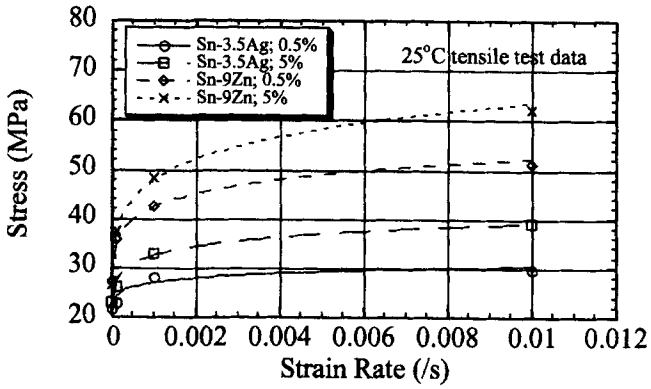

Fig. 3. Effect of strain rate on stress at different values of strain in Sn-Ag and Sn-Zn eutectics.

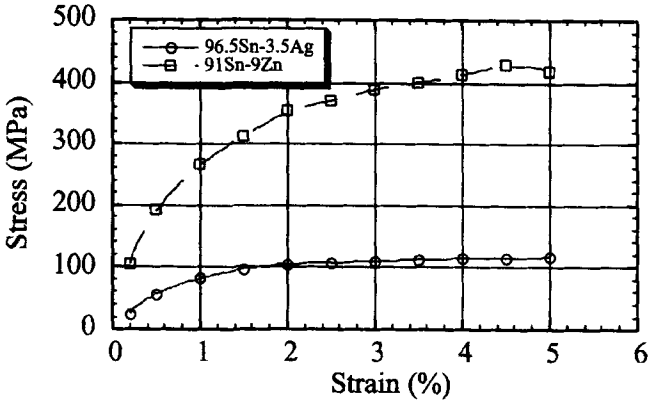

Fig. 4. Stress strain curves obtained by extrapolating from 25°C tensile data to strain rates high enough to suppress time-dependent effects on flow stress.

Table III. Parameters for the Dorn and Norton Equations from 25 and 80°C Tensile Data

		Dorn	Norton
96.5Sn-3.5Ag	A	5.83	6.62E-3
	n	12	12
	Q	111.2	108.5
91Sn-9Zn	A	8.22E + 3	9.27
	n	8.1	8.1
	Q	102.6	99.9

Note: Stress in MPa, strain rate in s^{-1} and Q in kJ/mole.

time for thermally activated processes. Since these thermally activated processes occur faster at higher temperatures, the stresses at corresponding strains are lower at 80°C than at 25°C. Table II summarizes the strain rate sensitivities (m), defined by the Eq. (5), at different temperatures and 5% total strain which is in the steady flow region.

$$\sigma = c_2 \dot{\varepsilon}^m \Big|_{\varepsilon,T} \qquad (5)$$

where c_2 is a constant and m is the strain rate sensitivity. As reported in literature,[12,13] the strain rate sensitivities increase with temperature for both solders. This increase is, however, small between 25 and 80°C.

The separation of plastic flow processes into an effectively rate independent stress strain curve and rate-dependent plastic flow processes (the latter consisting of thermally activated processes) is difficult; however, at a sufficiently high strain rate, depending on the time constants of the thermally activated processes, there is effectively a time independent stress strain curve (i.e., the activation energies for the processes involved such as cutting of forest dislocations by glide dislocations are very small). One way to get an approximate strain rate independent curve is to run tensile tests at different strain rates and extrapolate the flow stresses vs strain rate data at each value of strain to very high strain rates where the increase in flow stress with increasing strain rate becomes insignificant. Figure 3 shows the effect of strain rate on flow stress at two different values of strain obtained from the monotonic tensile curves shown in Figs. 2a and 2b. As can be seen, beyond a certain limit, increasing the strain rate would not cause significant increase in stress. Defining this stress to be the true unrelaxed stress for a given strain and determining these stresses at different values of strain allows us to get a stress-strain curve that is approximately "strain rate-independent" as discussed above. Such curves obtained by extrapolation from 25°C data for Sn-Ag and Sn-Zn are shown in Fig. 4. For this purpose, the unrelaxed stress is defined as corresponding to the point where the slope of the stress vs strain rate curve falls below 10^{-3} MPa-s. (The resolution of the testing machine is 10^{-2} MPa and therefore the value of 10^{-3} MPa-sec is chosen to be just below this resolution. Similar analysis is not shown for the 80°C data because a much faster strain rate is needed to approach the unrelaxed behavior.)

Both the Norton and the Dorn power laws [Eq. (1) and Eq. (3)] give good fits for the steady state flow stress vs strain rate data for Sn-Ag and Sn-Zn data at 25 and 80°C. The parameters obtained from the fits are summarized in Table III. The introduction of a threshold stress was not found necessary for a good fit; however, the exponents are not the theoretical values. The computed values from these fits are compared to experiment in Figs. 5a and 5b.

Creep Tests

Creep tests were performed in load control with initial stresses ranging from 10 to 22 MPa at two different temperatures, 25 and 80°C. A primary creep region was observed in all tests, unlike that reported for some superplastic materials. Power law type relationships between steady state secondary creep rates and stresses are observed (Fig. 6). The stress exponent for Sn-Ag is higher than for the Sn-Zn case. In the stress range investigated, a crossover is observed between the plots for eutectic Sn-Ag and Sn-Zn, i.e., at lower stresses, creep rates for Sn-Ag are found to be smaller than for Sn-Zn; however, as the stress is increased, the creep rate of Sn-Ag becomes faster than that of Sn-Zn.

The creep data for Sn-Ag and Sn-Zn eutectics at 25

and 80°C are seen to be well-described by both the Norton and the Dorn creep law formulae [Eq. (1) and Eq. (3)], with the values of the parameters summarized in Table IV. No threshold stress was found necessary to get a good fit although the n values for Sn-Ag eutectic are higher than the theoretical values. The close agreement between these fits and experimental results is shown in Figs. 7a and 7b.

Stress Relaxation Tests

Stress relaxation tests were performed in strain control. It was not necessary to account for machine compliance because strain rather than crosshead displacement was controlled. Loading times of 1 s were used and the specimens were held at different strains ranging from 0.3% to 2.4%. For the 80°C tests, the temperature was controlled to within ±1°C. Different specimens were used for each test. The percentage reduction in stress vs time is shown in Fig. 8a–8d. At 25°C, most of the stress is seen to relax rapidly in less than 120 s for both Sn-Ag and Sn-Zn eutectic. The stresses do not reduce all the way to zero, but level off at non-zero values. The stress relaxation thereafter was found to be insignificant (<1%) over a period of 24 h.

At 80°C, however, the stresses relax completely to zero in less than 24 h for all the cases. The 80°C tests

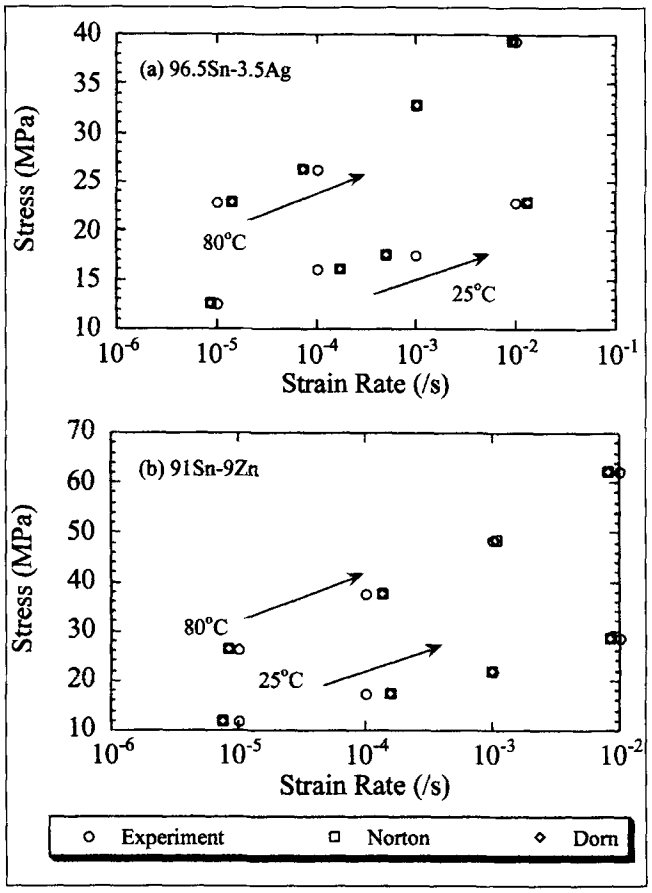

Fig. 5. Tensile data: Comparison of fits of Dorn and Norton equations for (a) Sn-Ag eutectic, and (b) Sn-Zn eutectic.

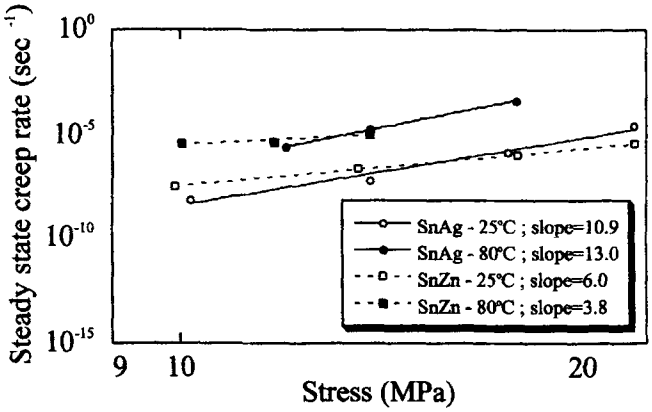

Fig. 6. Creep data for 96.5Sn–3.5Ag and 91Sn–9Zn at different stresses and temperatures (constant load tests).

Table IV. Parameters for the Dorn and Norton Equations from 25 and 80°C Creep Data

		Dorn	Norton
96.5Sn-3.5Ag	A	1.36E-3	1.50E-6
	n	11.3	11.3
	Q	82.3	79.5
91Sn-9Zn	A	1.91E + 1	2.17E-2
	n	5.7	5.7
	Q	68.0	65.2

Note: Stress in MPa, strain rate in s^{-1} and Q in kJ/mole.

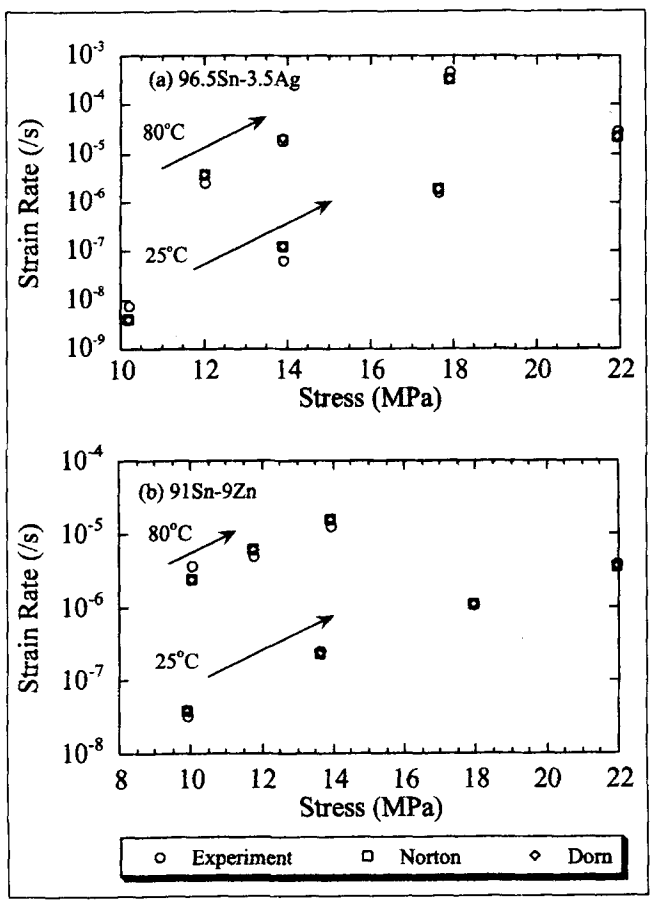

Fig. 7. Creep data: Comparison of fits of Dorn and Norton equations for (a) Sn-Ag eutectic, and (b) Sn-Zn eutectic

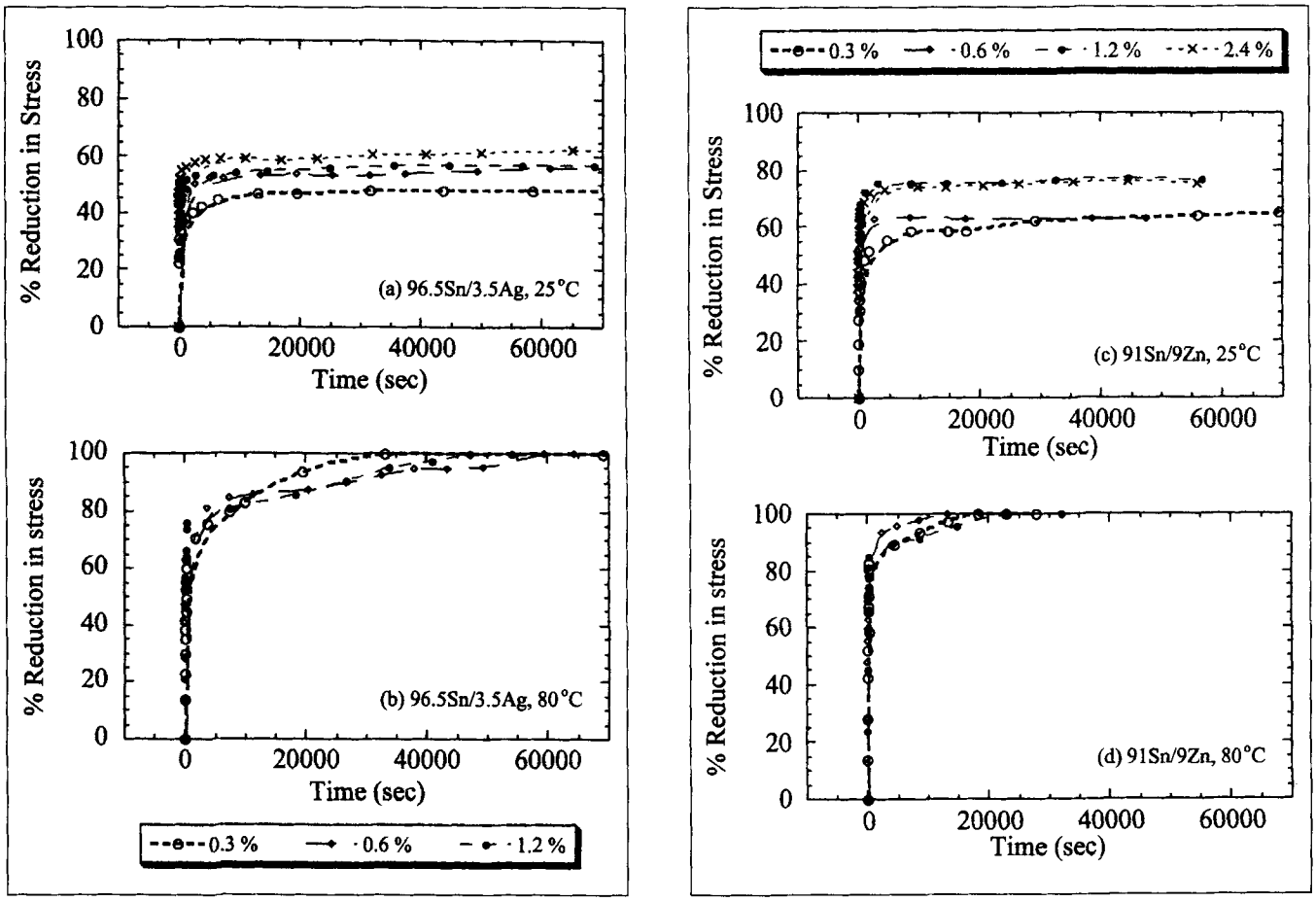

Fig. 8. Stress relaxation (% reduction from initial stress) at different values of total strain for (a) 96.5Sn–3.5Ag at 25°C, (b) 96.5Sn–3.5Ag at 80°C, (c) 91Sn–9Zn at 25°C, and (d) 91Sn–9Zn at 80°C.

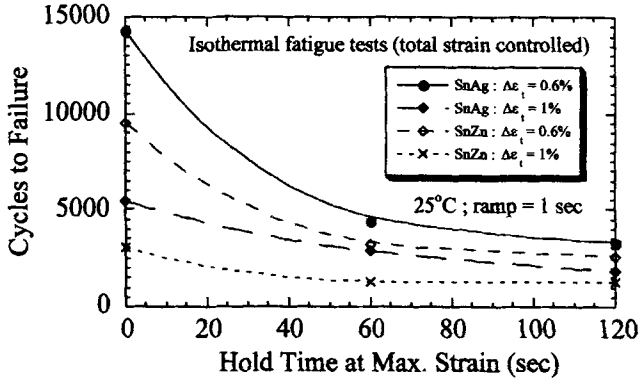

Fig. 9. Effect of hold time at maximum strain on isothermal fatigue lives of Sn-Ag and Sn-Zn eutectic solders at 25°C.

show two regions, first, a region of relatively rapid stress drop to a non-zero value of strain after which the stress relaxes at a lower rate all the way to zero stress. This suggests the operation of two mechanisms, the first with an activation energy low enough to cause relaxation at both at 25 and 80°C, and the second mechanism which comes into operation at 80°C allowing relaxation of stresses all the way to zero.

An interesting correlation is seen between the stress relaxation tests and isothermal strain-controlled fatigue tests at 25°C with hold time at maximum strain (with 1 s ramp time). The effect of hold time on these fatigue tests is to decrease the number of cycles to failure. However, a hold time of greater than 120 s was observed not to cause a further decrease in cycles to failure (Fig. 9). This correlates well with the fact that most of the stress in these solders has relaxed before 120 s. The authors suggest that during the hold time, damage accumulates in the form of slip steps at the surface (due to dislocations emerging out of the bulk). These slip steps play an integral part in the cracking process. Increasing hold time beyond 120 s does not cause further damage because the stress has relaxed to a low value.

The stress vs time curves at 25 and 80°C for both Sn-Ag and Sn-Zn are best described by a logarithmic decay law of the form:

$$\left(\frac{\sigma-\sigma_f}{\sigma_i-\sigma_f}\right)=A+B\ln t \qquad (6)$$

where σ is the instantaneous stress at time t, σ_i is the initial stress at the start of stress relaxation, σ_f is the final relaxed value of stress, A,B are constants, and t is the time. The relaxation times (time required for the stress to drop to 1/e of the stress drop seen in the region of rapid stress drop) decrease with increasing temperature and increasing strain (at which the speci-

men is held) for both Sn-Ag and Sn-Zn and were all less than 120 s.

The following approach was taken to treat the stress relaxation data. Since stress relaxation is a transformation from a high energy to a low energy state, it can be handled by a transformation kinetics type formulation. Stress relaxation at constant strain is driven by reduction in strain energy, $\sigma\varepsilon/2$. Thermally activated plastic flow occurs to reduce the internal energy. The rate of reduction in stress is proportional to the strain energy, a frequency factor, the amount of strain energy reduction per activated event, the dislocation density which controls the density of activated sites, and the probability that an attempt at an activated event is successful. The latter is given by $\exp(-\Delta G/RT)$ where for dislocation climb ΔG is the free energy of activation for creep. So, the governing equation may be written in the form:

Rate of energy change = constant × (driving force) × (no. of active sites) × (energy reduction per event) × (probability of successful event) or

$$\varepsilon\frac{d\sigma}{dt} = K(\varepsilon\sigma)(v\rho)(ab\sigma)\exp(-\Delta G/RT) \qquad (7)$$

where K is a constant, ε is the total strain (which is held constant during the stress relaxation), σ is the stress, v is the atomic vibration frequency, ρ is the dislocation density, a is the area swept by a dislocation per event, b is the Burgers vector, ΔG is the free energy change; ($\Delta G = \Delta H - T\Delta S$), ΔH is the change in enthalpy, ΔS is the change in entropy, R is the universal gas constant and T is the temperature.

Equation (7) can be rewritten in the general form:

$$\dot{\sigma} = A\sigma^n \exp(-Q/RT) \qquad (8)$$

where $\dot{\sigma}$ is the stress relaxation rate, A is a constant, and Q is the activation energy ($Q = \Delta H$). The value of n may vary depending on the dependence of ρ on σ and so on. The stress relaxation data was analyzed by extracting stress rate vs stress data from the stress vs time curves and relating this to a power law formulation. Since the stress relaxation curves show two distinct regions, one of rapid stress drop and another of relatively lower stress drop rate, a threshold stress σ_t is introduced into the equation to give:

$$\dot{\sigma} = A(\sigma - \sigma_t)^n \exp(-Q/RT) \qquad (9)$$

The fits for the Sn-Ag and Sn-Zn data at 25 and 80°C give the following values (averaged over the temperature and strain range investigated). For Sn-Ag, the stress exponent, threshold stress and activation energy are found to be 6, 9.8 MPa and 33.5 kJ/mole, respectively, while the values for Sn-Zn were 4.2, 3 MPa and 106.9 kJ/mole, respectively.

UNIFIED CREEP PLASTICITY MODELING

Toward the goal of incorporating the creep and plasticity effects of solders into a comprehensive model, the unified creep plasticity model[9,16] has been implemented for the various tests discussed before. The constitutive model is based on the dual backstress thermoviscoplasticity model proposed by McDowell et al.[9] The model accommodates temperature and strain-rate dependence, creep-plasticity interaction, and competitive hardening and recovery effects. The form of the flow rule is shown in Eq. (10) where the inelastic rate of deformation tensor (D_p) is composed of the viscous overstress (S_v which is a function of the deviatoric or traceless stress, the backstress state variable, and yield strength), drag strength (D) repre-

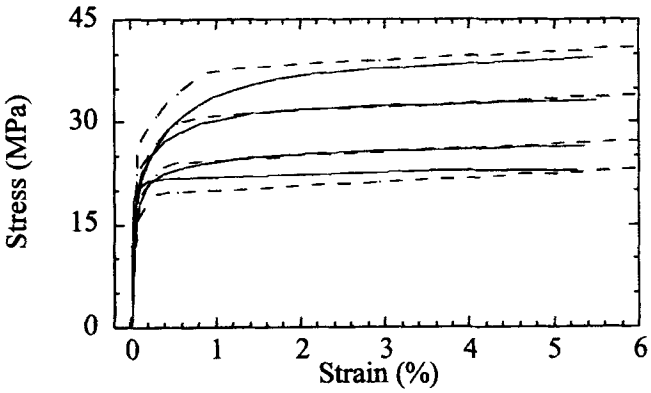

Fig. 10. Comparison of simulated (dashed lines) and experimental tensile test data for 96.5Sn–3.5Ag at 25°C for strain rates from 10^{-2} to 10^{-5}/s.

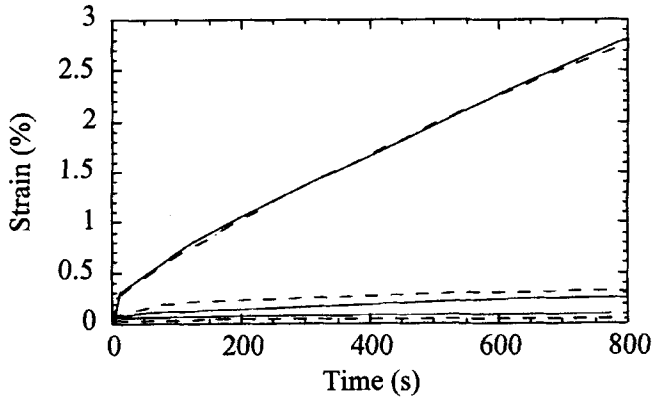

Fig. 11. Comparison of simulated (dashed lines) and experimental creep test data for 96.5Sn–3.5Ag at 25°C for various initial stresses.

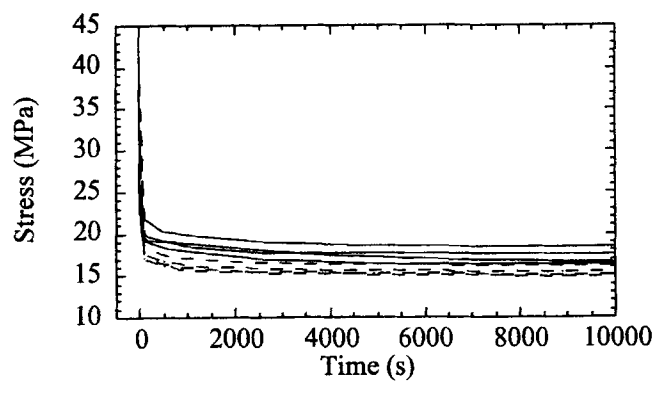

Fig. 12.Comparison of simulated (dashed lines) and experimental stress relaxation data 96.5Sn–3.5Ag at 25°C for strain ranges of 0.3, 0.6, 1.2, and 2.4%.

sentative of isotropic hardening, a thermal diffusivity (Θ), the strain direction (N) and constants A and B.

$$D^p = \sqrt{\frac{3}{2}} A \left(\frac{\langle S_v \rangle}{D} \right)^n \exp\left[B \left(\frac{\langle S_v \rangle}{D} \right)^{n+1} \right] \Theta N \qquad (10)$$

The simulations are compared with experimental values in Figs. 10–12. The agreement is found to be quite good.

CONCLUSIONS

The Dorn and Norton formulations [Eq. (1) and (3)] yield essentially the same values for the stress exponents. The activation energies obtained, however, differ because of the presence of the 1/T term. Since the exponential term dominates the 1/T term, this difference is small. The variation of the shear modulus μ with temperature would have an even smaller effect.

For 96.5Sn–3.5Ag, the tensile data yields values of stress exponent comparable to those derived from creep, suggesting that mechanisms similar to those occurring in creep are also responsible for the strain rate effects on tensile flow stress. This difference is slightly larger for the 91Sn–9Zn case. The values of Q and n obtained from creep tests for Sn-Zn agree very closely with the values Q = 64 kJ/mole and n = 6.2 reported by Hare and Stang[6] for the as-cast eutectic 63Sn–37Pb solder.

The activation energies obtained from the monotonic tensile tests for the Sn-Ag and Sn-Zn eutectics compare well with the activation energy for self-diffusion (approximately 100 kJ/mole) in pure lead and tin,[14,15] suggesting matrix creep mechanisms controlled by conventional dislocation climb. The high values of stress exponent could, however, mean that other mechanisms are operative simultaneously or that an effective stress term should be introduced.

The stress relaxation tests gave lower values of n than did the other two tests for the Sn-Ag and Sn-Zn eutectics, as well as a low value of Q for the Sn-Ag, suggesting either that different mechanisms are operating, or that a simple formulation like Eq. (9) is inadequate because of some of the terms in Eq. (7) having complex dependencies on stress and/or stress rate. An activation volume term needs to be introduced into the treatments but this makes the analysis and resulting equations much more complicated. Since the activation volume term subtracts from Q in the absence of a stress, the lower Q values from the stress relaxation experiments are not unexpected. The relaxation times in the stress relaxation tests were seen to decrease with increasing temperature and increasing strain. Since the stress relaxes to a constant value, the effects of hold time on isothermal fatigue also is expected to saturate as observed.

For purposes of modeling, a means of obtaining "time-independent" stress-strain curves, using an extrapolation scheme from tensile tests at different strain rates, has been suggested. The unified creep plasticity model, previously used to model high temperature super alloys, is able to give a very good fit for the tensile, stress relaxation and creep models simultaneously without having to change any parameters. This shows promise in incorporating it in a thermomechanical fatigue life prediction model that could prove useful in electronic device design.

REFERENCES

1. Z. Mei, J.W. Morris, Jr. and M.C. Shine, *J. Electron. Packaging* 113, 109 (1991).
2. D. Tribula and J.W. Morris, Jr., *J. Electron. Packaging,* 112, 87 (1990).
3. D.S. Stone, *J. Electron. Packaging* 112, 100 (1990).
4. J.K. Tien, B.C. Hendrix and A.I. Attarwala, *J. Electron. Packaging* 113, 115 (1991).
5. A.I. Attarwala, J.K. Tien, G.Y. Masada and G.Dody, *J. Electron. Packaging* 114, 109 (1992).
6. E.W. Hare and R.G. Stang, *J. Electron. Mater.* 24, 473 (1995).
7. G.S. Murty, *J. Mater. Sci.* 8, 611 (1973).
8. Z. Mei and J.W. Morris, *J. Electron. Mater.* 21, 599 (1992).
9. D.L. McDowell, M.P. Miller and D.C. Brooks, *ASTM STP 1153*, (Philadelphia, PA: ASTM, 1994), p. 42.
10. John H. Lau, ed., *Thermal Stress and Strain in Microelectronics Packaging*, (New York, NY: Van Nostrand Reinhold, 1993), p. 67.
11. Z. Guo, A.F. Sprecher and H. Conrad, *J. Electron. Packaging* 114, 112 (1992).
12. George E. Dieter, *Mechanical Metallurgy*, 3rd ed. (New York: McGraw-Hill, 1986), p. 295.
13. Robert E. Reed-Hill and Reza Abbaschian, *Physical Metallurgy Principles*, 3rd ed. (Boston: PWS-Kent Publishing Co., 1992), p. 836.
14. W. Lange and D. Bergner, *Phys. Stat. Sol.* 2, 1410 (1962).
15. N.H. Natchtrieb and G.S. Handler, *J. Chem. Phys.* 23, 1569 (1955).
16. H. Mavoori and J. Chin, *Proc. 45th Electronic Comp. and Tech. Conf.* 1, (New York: IEEE, 1995), p. 990.